Interactions between Polymers and Lipid Monolayers at the Air/Water Interface: Surface Behavior of Poly(methyl methacrylate)−Cholesterol Mixed Films

M. Miñones Conde,[‡] O. Conde,[†] J. M. Trillo,[†] and J. Miñones, Jr.*[,†]

Department of Physical Chemistry, Faculty of Pharmacy, and Department of Optometry, School of Optics and Optometry, University of Santiago de Compostela, Campus Sur, 15706-Santiago de Compostela, Spain

Received: April 16, 2010; Revised Manuscript Received: July 5, 2010

The behavior of mixed monolayers of cholesterol and poly(methyl methacrylate) (PMMA) with molecular weights of $M_w = 120\,000$ g/mol and $M_w = 15\,000$ g/mol was investigated at the air/water interface using Langmuir and Brewster angle microscopy techniques. From the data of surface pressure (π)−area (A) isotherms, compressional modulus−surface pressure ($C_s^{-1}-\pi$) curves, and film thickness, complemented with Brewster angle microscopy images, the interaction between the components was analyzed. Regardless of the surface pressure ($\pi = 10$, 20, or 30 mN/m) at which the mean molecular/monomer areas (Am) were calculated, the Am−mole fraction plots (corresponding to $X_{PMMA} = 0.1$, 0.3, 0.5, 0.7, and 0.9) show that all the experimental points obtained are placed on the theoretical straight line calculated according to the additivity rule. This fact, together with the existence of two collapses in the mixed monolayers and with the fact that the surface pressure of the *liquid-expanded* LE−L′E phase transition of PMMA does not change with the monolayer composition, demonstrates the immiscibility of the film components at the interface. The application of the Crisp phase rule to the phase diagram of PMMA−cholesterol mixed monolayers helps to explain the existence of a biphasic system, regardless of their composition and surface pressure. Besides, Brewster angle microscopy (BAM) images showed the existence of heterogeneous cholesterol domains with high reflectivity immersed in a homogeneous polymer separate phase with low reflectivity.

1. Introduction

Contact lenses are mainly intended for the correction of ametropia. The number of people who regularly wear contact lenses is exponentially increasing, and in the near future it is expected to surpass the number of those who wear traditional eyeglasses. On the other hand, the use of contact lenses as drug delivery systems is gaining increasing attention,[1] because of their therapeutic utility to meet certain demands, such as relief of ocular pain, promotion of corneal healing, mechanical protection, maintenance of corneal epithelial hydration, and, if medicated, drug delivery. The possibility exists to correct a vision problem and simultaneously treat an ocular disease pharmacologically.[1] Furthermore, the daily use of contact lenses involves a non-negligible risk, estimated to be 25% of the cases, of causing erosion and infections in the eye that could be reduced by the use of medical contact lenses.[2−4]

Many of the problems that arise from a continuous use of contact lenses can be caused by the interactions between the polymer of the contact lens and the components of the ocular tear. With the aim of obtaining further information about these interactions, the Langmuir film balance and Brewster angle microscopy techniques were used in this study. For this purpose, mixed monolayers made of poly(methyl methacrylate) (PMMA) and cholesterol were prepared. PMMA is a hard, resistant, transparent, acrylic material, with excellent optical characteristics and a high refractive index, which makes it suitable for the manufacture of rigid contact lenses. Besides, methyl methacrylate (MMA) monomer is also a main constituent of rigid gas-permeable contact lenses and of nonionic hydrophilic soft lenses of low and high hydration.[5−7]

On the other hand, the Langmuir cholesterol monolayer obtained at the air/water interface is similar to that of the tear lipids, because, according to Holly,[8] when raising the eyelids, the tear lipids spread and form a monolayer, which is destroyed in subsequent blinking. So, the Langmuir cholesterol monolayer can be an accurate model to study the behavior of the tear lipids. Moreover, the emergence of certain intolerance due to contact lenses and some components of the tear, such as cholesterol, was reflected in the literature.[9] High amounts of cholesterol in the tears of obese people, pregnant women during the first three months, and patients treated with diuretics led to fat deposition on their contact lenses, causing reduced vision and discomfort. High cholesterol levels in tears are correlated with high plasma cholesterol levels.

Despite cholesterol being a lipid widely studied in monolayers,[10] we believe our study is interesting and novel because the results obtained by Brewster angle microscopy (BAM) allow us to understand its morphology when participating in the mixed system formed by the contact lens and the tear. These results, together with those obtained from the analysis of surface pressure−area isotherms recorded as a consequence of the compression of mixed monolayers, will allow us to determine the behavior of the mixed monolayer, that is, whether there are any interactions between its components.

2. Experimental Section

Syndiotactic PMMAs of molecular weights $M_w = 15\,000$ g/mol and $M_w = 120\,000$ g/mol were purchased from Aldrich (purity 95%), while cholesterol was supplied from Sigma (purity 99%); all of them were used without further purification. These

* To whom correspondence should be addressed. Phone: +34 981 563100, ext. 14917. Fax: +34 981 594912. E-mail: qf.minones@usc.es.
[†] Department of Physical Chemistry.
[‡] Department of Optometry.

10.1021/jp103422g
Published on Web 08/02/2010

materials were stored according to the supplier information. Spreading solutions of 0.1−0.3 mg/mL were prepared using chloroform as a solvent. Only highly pure water, which was purified by means of a Milli-Q plus water purification system, with a resistivity of 18.2 MW·cm, was used in all experiments. The trough temperature was controlled by circulating constant temperature water from a Haake thermostat through the tubes attached to the aluminum-based plate of the trough. The subphase temperature was measured by a thermocouple located just below the air/water interface.

Surface pressure−area isotherms of PMMA (M_w = 120 000)−cholesterol mixed films were recorded with a KSV (Finland) Langmuir trough (total area = 850 cm^2) placed on an isolated vibration-free table and enclosed in a glass chamber to avoid contaminants from the air. The number of molecules spread on the water subphase was 1.5×10^{17}. After being spread, monolayers were left for 10 min to ensure the solvent evaporation. Compression was initiated with a barrier speed of 36 cm^2/min (2.4 Å^2 molecule^{-1} min^{-1}). Surface pressure was measured with the accuracy of ±0.1 mN/m using a Wilhelmy plate made from platinum foil as a pressure sensor.

To obtain surface pressure−area isotherms of syndiotactic PMMA (M_w = 15 000)−cholesterol mixed monolayers and to observe their morphological characteristics by Brewster angle microscopy (BAM), experiments were carried out with a Nima 601 trough (Coventry, UK) placed on a antivibration table. The trough has a working area of 70 cm ×7 cm, which is large enough to directly mount the BAM. Surface pressure was measured with the accuracy of ±0.1 mN/m using a Wilhelmy plate made from chromatography paper as the pressure sensor. The number of molecules spread on the water subphase was 8.82×10^{16} to ensure that the initial molecular area will be the same as that for the PMMA (120 000)−cholesterol system mentioned above. After being spread, monolayers were left for 10 min to ensure the solvent evaporation, after which compression was initiated with a barrier speed of 36 cm^2/min (4.1 Å^2 molecule^{-1} min^{-1}).

BAM images and ellipsometric measurements were performed with BAM 2 Plus (NFT, Göttingen, Germany) equipped with a 30 mW laser emitting p-polarized light with a wavelength of 532 nm which was reflected off the air/water interface at approximately 53.1° (incident Brewster angle). Under such conditions, the reflectivity of the beam was almost zero on the clean water surface. The reflected beam passes through a focal lens into a analyzer at a known angle of incident polarization and finally to a CCD camera. To measure the relative thickness of the film, a camera calibration was necessary previously in order to determine the relationship between the gray level (GL) (intensity unit) and the relative reflectivity (I), according to the procedure described by Rodríguez Patino et al.[11] The light intensity at each point in the BAM image depends on the local thickness and film optical properties. These parameters can be measured by determining the light intensity at the camera and analyzing the polarization state of the reflected light by the method based on Fresnel equations. At the Brewster angle:

$$I = |R_p^2| = C \times d^2$$

where I is the relative reflectivity (defined as the ratio of the reflected intensity (I_r) and the incident intensity (I_0), $I = I_r/I_0$), R_p is the p-component of the light, C is a constant, and d is the film thickness.

The lateral resolution of the microscope was 2 μm, the shutter speed used was 1/50 s, and the images were digitized and processed to optimize image quality; those shown below correspond to 768 × 572 pixels.

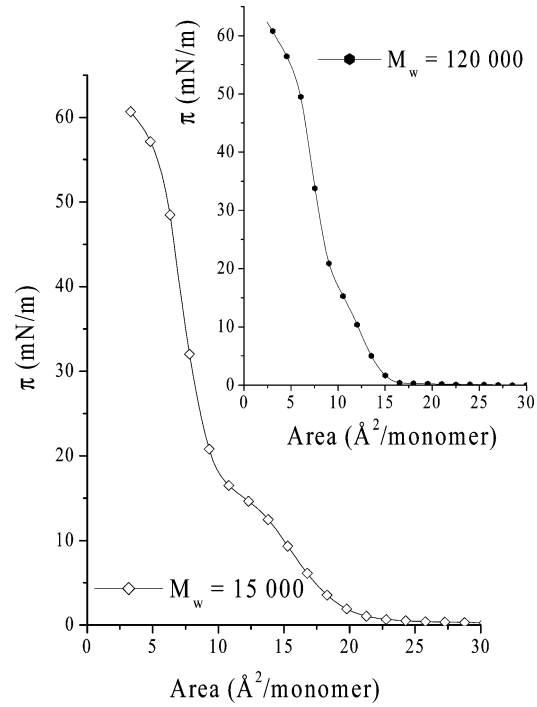

Figure 1. Surface pressure (π)−area (A) isotherms of PMMA (M_w = 15 000) and PMMA (M_w = 120 000) monolayers spread on water, pH 6, at 30−35 °C. Number of spread molecules: 1.5×10^{17}. Rate of compression: 2.4 Å^2 monomer^{-1} min^{-1}.

3. Results

3.1. Monolayers of Pure Components. In order to study the influence of PMMA molecular weight on mixed monolayer behavior, two polymers with different molecular weight were used: one of M_w = 15 000 g/mol (150 monomers) and another of M_w = 120 000 g/mol (1200 monomers), spread on water of pH = 6 at a temperature range of 30−35 °C. The corresponding isotherms of both polymer monolayers are slightly different (Figure 1). PMMA (15 000) occupies a larger area than PMMA (120 000). Indeed, the limiting area, A_0 (area extrapolated to zero surface pressure), corresponding to the first polymer is about 20 Å^2/monomer, and, in this situation, the monolayer exhibits an expanded state. Such value (corresponding to 1.2 m^2/mg) matches the calculated area from molecular models for the polymer in their trans configuration.[12,13] The value of the limiting area for PMMA (120 000) is lower than for PMMA (15 000), showing a less compressible monolayer (higher rigidity)[14] (inset of Figure 1).

From our point of view, the plateau observed in the $\pi-A$ isotherms of both polymers correspond to a LE−L′E phase transition from a *liquid-expanded* (LE) to another *liquid-expanded* (LE′) state of the monolayers.[14] The plateau (or pseudoplateau) is more pronounced (longer and flatter) for PMMA (15 000), although the transition pressure value is the same for both polymers (15−17 mN/m). Similar values were obtained by Brinkhuis and Schouten[15] for a PMMA polymer with molecular weight of 46 000 g/mol. Also, Hsu et al.[16] point out a value of 15.8 mN/m for the surface pressure of the plateau at 25 °C in the case of *synd*-PMMA polymer of molecular weight 100 000 g/mol.

The corresponding $\pi-A$ isotherm for cholesterol (Figure 2) was obtained on water of pH 6 at 30 °C. This temperature is

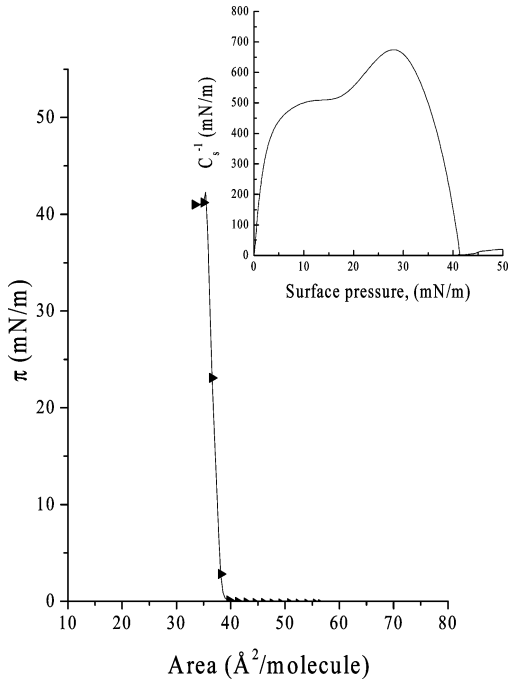

Figure 2. Surface pressure (π)−area (A) curve of cholesterol monolayer spread on water (pH 6 at 30 °C). Inset: Compressional modulus (C_s^{-1}) vs surface pressure (π) curve. Number of spread molecules: 1.5×10^{17}. Rate of compression: 2.4 Å^2 molecule^{-1} min^{-1}.

lower than that of the tear (32−35 °C)[17] but, according to Baglioni et al.,[18] the spreading isotherms of cholesterol are temperature independent in the range of 15−45 °C, within the experimental error. Cholesterol exhibits a condensed film, and the area extrapolated to zero surface pressure is around 38.5 Å^2/molec. Similar values were reported in the literature. Thus, a value of 37.8 Å^2/molec was achieved by Ries et al.,[19] while Müller et al.[20] and Motomura et al.[21] reported values of 38.4 Å^2/molec and 38.5 Å^2/molec, respectively.

The physical state of a monolayer and its collapse surface pressure value can be determined in a more precise way (compared to the π−A isotherms) with the plot of the compressional modulus ($C_s^{-1} = -A(\partial\pi)/(\partial A)$) as a function of surface pressure. The $C_s^{-1}-\pi$ curve for cholesterol shows a pronounced maximum, with C_s^{-1} values about 700 mN/m (inset of Figure 2). According to Davies and Rideal,[22] these values are characteristic of a very rigid structure, typical of a surface *solid* state. Similar values were reported by Baglioni et al.[18] and by other researchers.[23,24]

The π value (42.1 mN/m) corresponding to $C_s^{-1} = 0$ ($\pi_{collapse}$) is observed with precision in the $C_s^{-1}-\pi$ curve. As the measured equilibrium spreading pressure obtained by us was 38 mN/m (which is in agreement with previously reported values of 36 mN/m[25] or 39.9 mN/m[26]), the initial experimental collapse pressure value obtained here (42.1 mN/m) demonstrates that the monolayer in this region is in an unstable state, which is rapidly transformed into another collapsed phase that is in equilibrium with the monolayer at a lower surface pressure.[27]

3.2. Mixed Monolayers of PMMA (120 000)−Cholesterol. Surface Pressure (π)−Area (A) Isotherms and $C_s^{-1}-\pi$ Curves. Figure 3A shows the $\pi-A$ isotherms of pure PMMA (molecular weight, $M_w = 120\,000$ g/mol), pure cholesterol, and their mixtures of mole fractions $X_{PMMA} = 0.1$, 0.3, 0.5, 0.7, and 0.9, spread at 30 °C on the aqueous subphase at pH 6. The pure cholesterol and $X_{PMMA} = 0.1$ mixture exhibit rigid monolayers at all surface pressures, as they correspond to films in a *solid* state. For other mixtures, the monolayers are more expanded and show the characteristic LE−L′E transition region of PMMA.[14] This region can be observed more clearly in the $C_s^{-1}-\pi$ curves (Figure 3B). Except for the mixture of mole fraction $X_{PMMA} = 0.1$, the other $C_s^{-1}-\pi$ curves show the existence of a clear minimum attributed to the LE−L′E polymer phase transition, which corresponds to the existence of the plateau observed in the $\pi-A$ curves. The plateau surface pressure (14−15 mN/m) is practically constant for all mixtures (Table 1).

Another significant characteristic of these mixed monolayers is the existence of two collapses: the first, at about 42−43 mN/m, coincides with that of pure cholesterol, and the second, at a surface pressure about 60 mN/m, matches that of pure PMMA. These two collapses can be clearly seen in the curves corresponding to the monolayers of composition $X_{PMMA} = 0.1-0.5$. When the polymer content is 0.7 and 0.9, only a sharp cholesterol collapse is observed. In this situation, as the monolayer is compressed, the surface pressure increases, but the corresponding collapse of PMMA is not clearly shown in the $\pi-A$ curves. However, in the $C_s^{-1}-\pi$ curves, two minimum points at higher pressures (marked with arrows in the Figure 3B), corresponding to the two collapses, were clearly observed. This demonstrates the importance of the compressional modulus plots, which allow the observation of monolayer collapse, which cannot be visualized in the corresponding compression isotherms. The surface pressure values obtained for the two collapses are shown in Table 1.

3.3. Mixed Monolayers of PMMA (15 000)−Cholesterol. Surface Pressure (π)−Area (A) Isotherms and $C_s^{-1}-\pi$ Curves. A similar behavior to the one described above is observed when the mixed monolayers are made of PMMA (15 000) (Figure 4A). The mixed monolayer of $X_{PMMA} = 0.1$, similar to that of cholesterol, is very rigid. However, the mixed films corresponding to the remaining mole fractions are more expanded, showing their π−A isotherms (at surface pressures between 13.5 and 15 mN/m, Table 2), the typical discontinuity corresponding to the phase transition LE−L′E of the pure PMMA monolayer, as previously described.

All mixed monolayers exhibit values for the collapse surface pressure ranging approximately between 42 and 44 mN/m, which practically coincides with that of pure cholesterol film. Once the first collapse is reached, the surface pressure raises as the monolayer is compressed, without clearly observing the second collapse, as in the case of the PMMA (120 000)−cholesterol system studied previously.

In Figure 4B the values of the compressional modulus (C_s^{-1}) were plotted as a function of surface pressure (π). Similarly to PMMA (120 000), the polymer addition to the cholesterol causes a more elastic film, with two maximum values in $C_s^{-1}-\pi$ curves at, approximately, 7.5 mN/m and 25 mN/m, respectively. Between both maxima there is a point where the C_s^{-1} values show a minimum at about 15 mN/m, which corresponds to the discontinuity in the π−A curve of pure PMMA, relative to the LE−L′E transition.

3.4. Mean Molecular Area vs Mole Fraction Plots. Undoubtedly, the mean molecular area−mole fraction plots allows better estimation for the existence (or the absence) of interactions between mixed monolayers components, in comparison to $\pi-A$ isotherms. In order to create these plots, mean molecular/monomer area values (Am) corresponding to three surface pressures were chosen: at $\pi = 10$ mN/m, below the phase transition LE−L′E; at 20 mN/m, above the transition region; at 35 mN/m, close to the collapse of cholesterol.

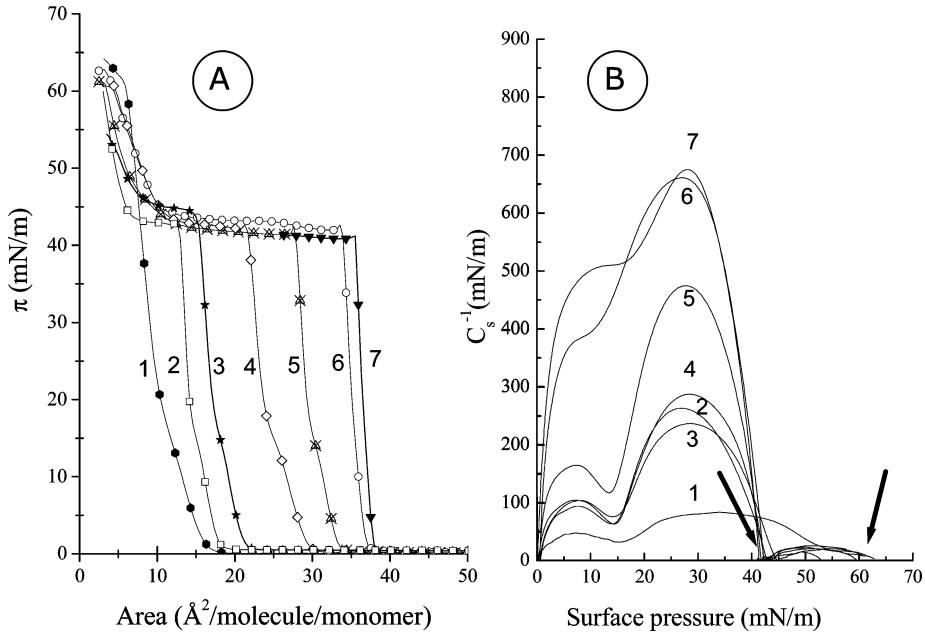

Figure 3. (A) Surface pressure (π)−area (A) isotherms for pure components and for PMMA (120 000)−cholesterol mixed monolayers spread on water (pH = 6 at 30 °C). (B) Compressional modulus (C_s^{-1})−surface pressure (π) plots for pure and mixed monolayers. Symbols: 1, PMMA; 2 to 6, X_{PMMA} = 0.9 to 0.1; 7, cholesterol. Number of spread molecules: 1.5×10^{17}. Rate of compression: 2.4 Å^2 molecule^{-1} (monomer^{-1}) min^{-1}.

TABLE 1: Surface Values Corresponding to Different Phase Transitions of PMMA (120000)−Cholesterol Mixed Monolayer Spread on Water at pH 6 and 30 °C

X_{PMMA}	phase transition (mN/m)	first collapse (mN/m)	second collapse (mN/m)
0		41.5	
0.1		42.0	62.7
0.3	13.5	41.7	62.6
0.5	14.0	42.3	59.5
0.7	13.8	43.5	59.0
0.9	14.0	42.6	62.4
1	15.0		62.4

Figure 5A and 5B shows the results corresponding to PMMA (120 000)−cholesterol and PMMA (15 000)−cholesterol mixed systems, respectively. At all values of surface pressure (π = 10, 20, or 30 mN/m), Am−X_{PMMA} plots show that all experimental points are situated in a straight line (discontinuous lines of Figure 5) calculated according to the additivity rule (Am = $X_{PMMA}A_{PMMA} + X_{chol}A_{chol}$). This behavior is typical for ideal mixed monolayers made of miscible components or for systems of immiscible constituents at the air/water interface.

3.5. Brewster Angle Microscopy (BAM). For PMMA (15 000)−cholesterol mixed monolayers with mole fractions of X_{PMMA} = 0.1, 0.3 and 0.5, the results obtained from $d-t$ (thickness−time) plots and the corresponding BAM images for different surface pressure values were very similar. Figure 6 shows that for the mixture of mole fraction X_{PMMA} = 0.5, the initial thickness monolayer is only about 0.5 nm, the same as for X_{PMMA} = 0.1 and 0.3 (for brevity, results are not shown). In this region, there is an important number of noise peaks with a high intensity in the $d-t$ curves, which are caused by the existence of big "elliptic vacuoles" of cholesterol (inset A of Figure 6). Approximately 300 s after the beginning of compression the film thickness rises abruptly, reaching a value about 2 nm without the presence of noise peaks as a consequence of "elliptic vacuole" disappearance on behalf of the formation of a homogeneous region (inset B of Figure 6). When cholesterol collapse is reached, noise peaks can be observed again on the thickness curve, raising the thickness up to about 3 nm (Figure 6). In this situation, small and bright "stripes" of collapsed monolayer can be seen (insets C and D of Figure 6).

PMMA (15 000)−cholesterol (X_{PMMA} = 0.7) and pure PMMA $d-t$ plots are shown in Figure 7. The thickness curve behavior for the mixed monolayer is very similar to that for the pure PMMA. As previously mentioned, thickness mixed monolayer is only 0.5 nm at the beginning of compression, remaining constant up to 300 s. In this region the $d-t$ curve shows the existence of low-intensity noise peaks because of the presence of small and slightly circular domains of cholesterol which can be seen in the image corresponding to this region (inset A of Figure 7) floating on a gray bottom made of PMMA monolayer. At 300 s after the beginning of compression, a detectable increase of mixed monolayer thickness originates, in a way similar to that of the mixture discussed above. As the compression is continued, the thickness curve shows a pseudoplateau with values between 1 and 2 nm. Then there is a continuous increase in thickness, reaching a value of about 8 nm, until collapse. In this region of the $d-t$ curve, the existence of noise peaks are hardly observed, due to the practically homogeneous structure of the monolayer as a consequence of packed cholesterol domains, as seen in the BAM images obtained under such conditions (inset B of Figure 7). However, as usual, as cholesterol collapse is reached, noise peaks appear again as a consequence of the collapsed tridimensional structures of cholesterol, which can be observed in inset C of Figure 7.

Evolution in time of the thickness of PMMA−cholesterol (X_{PMMA} = 0.9) mixed monolayer together with that of pure PMMA, is shown in Figure 8. The relative thickness curve of mixed monolayer practically coincides with that obtained for pure PMMA in a similar way to the previously discussed mixture; only there are some noise peaks in comparison with pure PMMA. The corresponding BAM images can be seen in the inset of Figure 8. All of them show the characteristic homogeneity of liquid expanded films, as corresponded to the pure PMMA monolayer. Only in a few cases (inset B) small and very poor cholesterol domains with high reflectivity can be detected. Even when the cholesterol collapse is reached, it

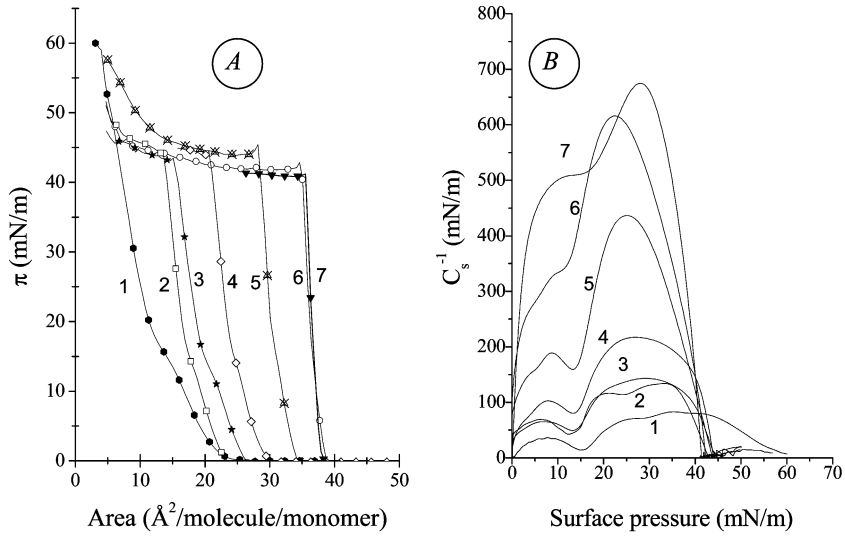

Figure 4. (A) Surface pressure (π)−area (A) isotherms for pure components and for PMMA (15 000)−cholesterol mixed monolayers spread on water (pH = 6 at 30 °C). (B) Compressional modulus (C_s^{-1})−surface pressure (π) plots for pure and mixed monolayers. Symbols: 1 PMMA; 2 to 6, $X_{PMMA} = 0.9$ to 0.1; 7. Cholesterol. Number of spread molecules: 8.8×10^{16}. Rate of compression: 4.1 Å^2 molecule^{-1} (monomer^{-1}) min^{-1}.

TABLE 2: Surface Values Corresponding to Different Phase Transitions of PMMA (15000)−Cholesterol Mixed Monolayer Spread on Water at pH 6 and 30 °C

X_{PMMA}	phase transition (mN/m)	first collapse (mN/m)
0		43.2
0.1		42.2
0.3	13.4	43.7
0.5	13.4	43.8
0.7	13.1	42.8
0.9	13.2	43.8
1	14.9	

is not possible to observe their typical structures, like stripes or compacted masses of the collapsed monolayer (inset C).

4. Discussion

The existence of two collapses in the mixed monolayers at the same surface pressure corresponding to the collapse of each pure component is typical of systems made of immiscible components in the air−water (A/W) interface.[28,29] However, the incompatibility of the components in the region of collapse does not necessarily mean that they are also immiscible at lower surface pressures. In the literature there are results for various systems in which components are miscible at low surface pressures but not at higher pressures. Such is the case for mixtures of cholesterol with carotenes, studied by Chifu et al.[30] Similarly, Motomura et al.[31] conclude that the components of the systems made of cholesterol and fatty acids are miscible when a mixed monolayer is in an *expanded state* (low surface pressures) and immiscible in the *condensed state* (high surface pressures). Similar results were obtained by Albrecht et al.[32] when studying mixtures of dipalmitoyl and dimyristoyl phosphatidyl choline with cholesterol. In the same way, the surface pressure−area isotherms for poly(benzyl methacrylate) and arachidic acid, investigated by Nordli Borve,[33] show the compatibility of the two components at low surface pressures and their incompatibility at high pressures. Recently, our studies have also shown that at surface pressures below 20 mN/m, amphotericin B (AmB) is compatible with dipalmitoyl phosphatidyl serine (DPPS) monolayer, but when the surface pressure exceeds 20 mN/m, both components give rise to two separate phases.[34]

Miscibility or immiscibility of the components of mixtures of PMMA and cholesterol, regardless of their surface pressure, can be evaluated using the Crisp phase rule[28] applied to bidimensional systems.[35−37] On the assumption that temperature and pressure (atmospheric) remain constant, the degrees of freedom, as defined by the rule of the phases in the case of a monolayer, are $L = C - F + 1$ (eq 1), where C is the number of components and F is the number of phases (except air and water). Therefore, in our system, $C = 2$ (PMMA and cholesterol) and $F = 3 - L$ (eq 2).

The phase diagram for this system, obtained with the data of Table 1, is shown in Figure 9. Along the horizontal lines of this figure, the surface pressure remains constant, regardless of the composition of the mixed monolayer, so that in eq 2, $L = 0$ and consequently $F = 3$, i.e., three phases in equilibrium coexist on the horizontal lines of the phase diagram. To explain the nature of these phases, three assumptions can be made:

(1) In region A of the phase diagram (at pressures below the transition phase), there is a homogeneous mixed monolayer constituted by miscible components forming a single phase with $PMMA_{(h)}$, molecules, horizontally oriented on the water surface, and cholesterol molecules, vertically oriented ($Chol_{(v)}$). In region B, the mixed monolayer components are separated into two different phases: one consisting of cholesterol split from the previous system, and another one by the molecules of $PMMA_{(l)}$ which, as a result of the phase transition carried out at 13−14 mN/m, change their orientation from the horizontal position to a coiled configuration due to the folding of the polymer segments, forming loops at the interface,[14] and thus creating a separate phase from cholesterol.

(2) Unlike the previous proposal, in region A of the phase diagram the components are immiscible while in region B they are miscible.

(3) In both regions of the phase diagram, there is immiscibility of the components: in the first case, the system consists of molecules of $PMMA_{(h)}$ incompatible with those of cholesterol ($Chol_{(v)}$), and in the second region this component is also incompatible with folded $PMMA_{(l)}$, forming loops at the interface.

With regard to the first hypothesis, it is difficult to imagine that the horizontally oriented PMMA molecules on the aqueous subphase can form a miscible system with cholesterol, which

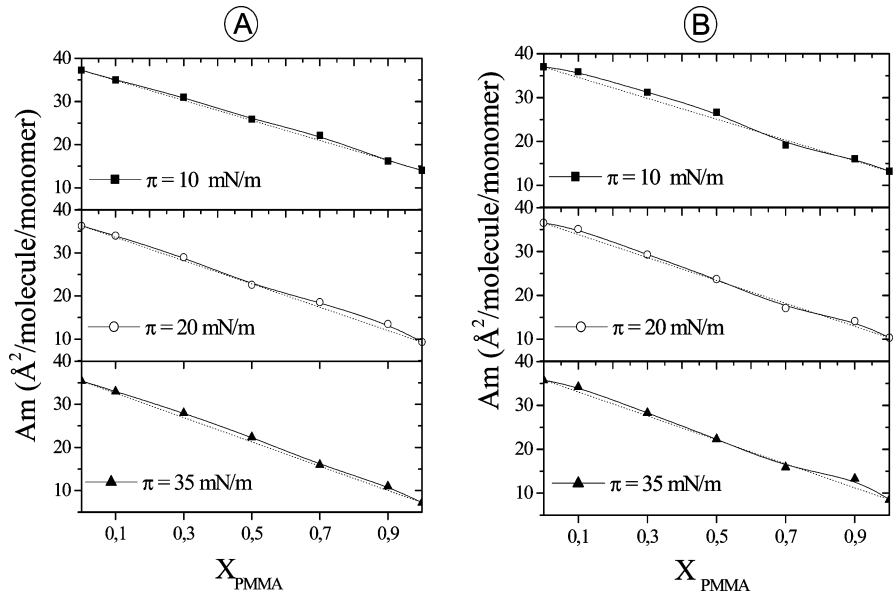

Figure 5. Mean molecular area (Am) vs mole fraction (X_{PMMA}) plots for mixed monolayers of PMMA and cholesterol at different surface pressures. (A) PMMA (120 000). (B) PMMA (15 000). Subphase: water (pH = 6 at 30 °C). Dashed lines: theoretical lines obtained according to the additivity rule. Solid lines: experimental results.

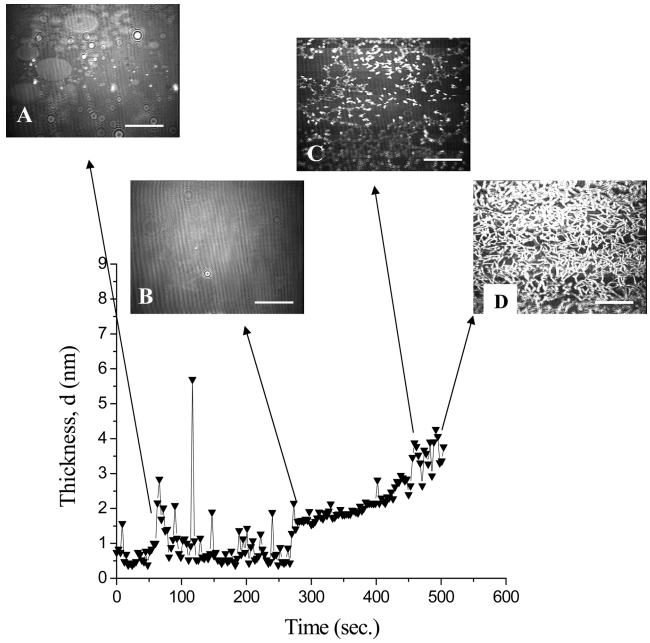

Figure 6. Thickness (d)−time (t) plot corresponding to PMMA (15 000)−cholesterol mixed monolayer ($X_{PMMA} = 0.5$) spread on water (pH 6 and 30 °C). Inset: BAM images at different surface pressures. (A) At $\pi = 0.9$ mN/m. (B) At $\pi = 16$ mN/m. (C and D) At $\pi = 42$ mN/m (cholesterol collapse). Scale bar: 20 μm.

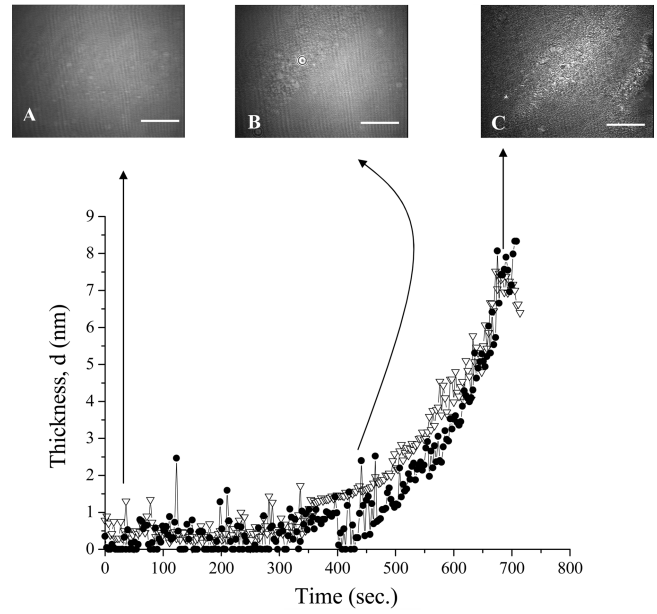

Figure 7. Thickness (d)−time (t) plot corresponding to the PMMA (15 000)−cholesterol mixed monolayer of composition $X_{PMMA} = 0.7$ (▽) and the pure monolayer of PMMA (●). Inset: BAM images at different surface pressures. (A) At $\pi = 3.5$ mN/m. (B) At $\pi = 10$ mN/m. (C) At $\pi = 44.5$ mN/m. Scale bar: 20 μm.

is anchored vertically in the water through the 3β-hydroxyl group. Indeed, in the literature there have been numerous examples of systems made of immiscible components as a consequence of their different orientation at the A/W interface. Thus, the mixture studied by Nakagaki et al.,[38] consisting of 16-(9-anthroyloxy)palmitic acid oriented horizontally at low surface pressures, and cholesterol, oriented vertically, shows the incompatibility of these components at the interface. Likewise, several authors[39−42] have found that mixed monolayers of PMMA and fatty acids are immiscible as a result of their different orientation at the water surface, although Peng and Barnes[43] were skeptical about the validity of these results (collapse pressure and molecular areas) on which the authors based their conclusions.

Similarly, in systems made of components different from those studied by us, immiscibility has been demonstrated between monolayers because of their different orientations in the interface. Thus, the results of Niccolai et al.,[44] related to mixed monolayers of 1-glycerol monooleoil (MON) and 1-glycerol monoestearoil (MOS), confirm the "empirical rule" that immiscibility of the components at the interface is due to their different orientations (MON, horizontal; MOS, vertical). Other authors[45,46] attribute the miscibility or immiscibility of the components to the physical state of their respective monolayers: when both are in the same surface state (for example in the expanded state), components are miscible at the

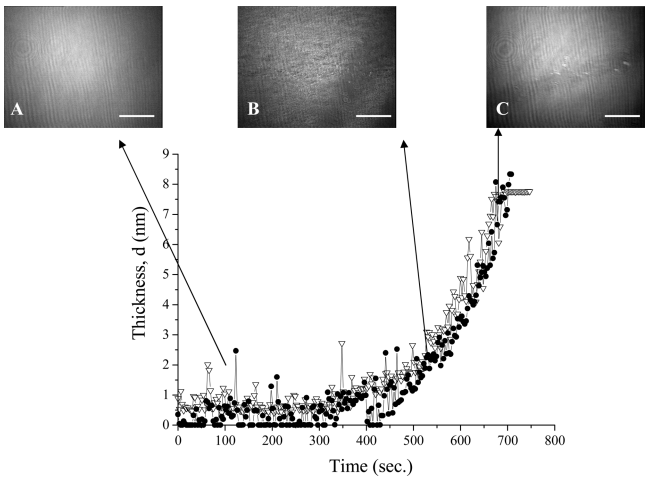

Figure 8. Thickness (d)−time (t) plot corresponding to the mixed monolayer of PMMA (15 000)−cholesterol of composition $X_{PMMA} = 0.9$ (▽) and the pure monolayer of PMMA (●). Inset: BAM images at different surface pressures. (A) At $\pi = 0$ mN/m. (B) At $\pi = 9.7$ mN/m. (C) At $\pi = 43.9$ mN/m. Scale bar: 20 μm.

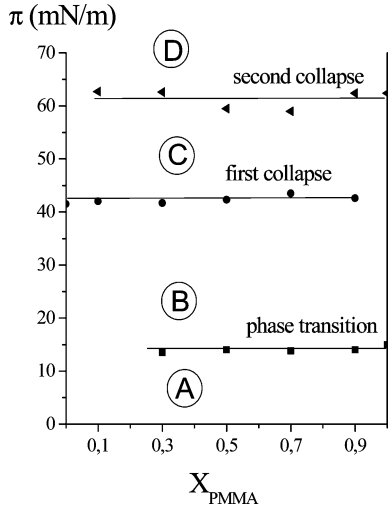

Figure 9. Phase diagram of mixed monolayers of PMMA (120 000)−cholesterol obtained from the data of Table 1.

interface, whereas if they are in different surface states (for example, liquid-expanded and liquid-condensed states), they are partially miscible or immiscible. In fact, this reference to the physical states of the monolayer is another way of considering the different orientations of the molecules at the interface, because the nature of the surface state depends on the arrangement of molecules on the water surface.

Therefore, in accordance with these results, it is postulated that in region A of the phase diagram there are two immiscible phases formed by $PMMA_{(h)}$, horizontally oriented, and by cholesterol ($Chol_{(v)}$), vertically oriented. Similarly, in region B, cholesterol ($Chol_{(v)}$) originates an incompatible system with the folded $PMMA_{(l)}$, resulting from the LE−L′E phase transition of this compound. In short, on the first horizontal line of the phase diagram of Figure 9, the three phases in equilibrium are those proposed in the third above-mentioned hypothesis. The linearity of the results obtained from the mean molecular area versus mole fraction of PMMA plots (Figure 5) contributes to support this hypothesis.

The second horizontal line of the phase diagram, at surface pressures of 41−42 mN/m, corresponds to the collapse of cholesterol ($Chol_{(collapse)}$), while the third line, at $\pi = 62$ mN/m, coincides with the collapse of $PMMA_{(l)}$. The independence of the collapse surface pressures from the composition of the monolayers is evidence that cholesterol is immiscible with PMMA. Consequently, on the second horizontal line of the phase diagram, the three phases in equilibrium are constituted by (a) cholesterol ($Chol_{(v)}$), (b) folded $PMMA_{(l)}$, and (c) collapsed cholesterol ($Chol_{(collapsed)}$). Similarly, along the third horizontal line there are also three phases coexisting in equilibrium: (a) folded $PMMA_{(l)}$, (b) collapsed cholesterol ($Chol_{(collapsed)}$), and (c) collapsed polymer ($PMMA_{(l)\ collapsed}$). A similar reasoning applied to the PMMA (120 000)−cholesterol system can be extrapolated to the mixed films of PMMA (15 000)−cholesterol because their surface behavior is practically the same.

5. Conclusions

Mean molecular area−mole fraction plots corresponding to PMMA (120 000)−cholesterol and PMMA (15 000)−cholesterol mixed systems show that all experimental points are situated in a straight line calculated according to the additivity rule. This behavior is typical for ideal mixed monolayers made of miscible components or for systems of immiscible constituents at the air/water interface. However, the existence of two collapses in the mixed monolayers at the same surface pressure corresponding to the collapse of each pure component as well as the fact that the surface pressure corresponding to the LE−L′E phase transition does not vary with mixed monolayers composition are characteristic of systems made of immiscible components. In short, one can speculate that there is no interaction between the contact lenses made of PMMA and the cholesterol of the tear. Consequently, the existence of certain intolerance between contact lenses and some components of tears, such as cholesterol, as was reflected in the literature, does not seem to be caused by an interaction between both components, because they are immiscible at the air/tear interface.

Acknowledgment. We acknowledge the support of the Xunta de Galicia (Spain) through project number PGIDIT07PXIB-203133PR.

References and Notes

(1) Alvarez Lorenzo, C.; Hiratani, H.; Concheiro, A. *Am. J. Drug Delivery* **2006**, *4* (3), 131.
(2) Vandorselaer, T.; Youssfi, H.; Caspers-Valu, L. E.; Dumont, P.; Vauthier, L. *J. Fr. Ophthalmol.* **2001**, *24*, 1025.
(3) Lesher, G. A.; Gunderson, G. G. *Optom. Vis. Sci.* **1993**, *70*, 1012.
(4) Salz, J. J.; Reader, A. L.; Schwartz, L. J.; Van Le, K. *J. Refract. Corneal Surg.* **1994**, *10*, 640.
(5) Feinbloom, W. *Am. J. Optom.* **1937**, *14*, 41.
(6) Tuhoy, K. M. U.S. Patent 2510438, 1948.
(7) Dickinson, F. *Optician.* **1954**, *128*, 493.
(8) Holly, F. J. *Opthalmol. Clin.* **1973**, *13*, 73–86.
(9) Young, W. H.; Hill, R. M. *Am. J. Optom.* **1973**, *50*, 12–16.
(10) Gaines, G. L., Jr. *Insoluble Monolayers at Liquid/Gas Interfaces*; Prigogine, I., Ed.; Interscience Publishers: New York, 1966; pp 254−264.
(11) Rodriguez Patino, J. M.; Sánchez, C. C.; Rodríguez Niño, M. R. *Langmuir* **1999**, *15*, 2484.
(12) Peng, J. B.; Barnes, G. T. *Langmuir.* **1991**, *7*, 1749.
(13) Labbauf, A.; Zack, J. R. *J. Colloid Interface Sci.* **1971**, *35*, 569.
(14) Miñones, J., Jr.; Miñones Conde, M.; Yebra-Pimentel, E.; Miñones Trillo, J. *J. Phys. Chem. C* **2009**, *1123*, 17455.
(15) Brinkhuis, R. H. G.; Schouten, A. J. *Langmuir* **1992**, *8*, 2247.
(16) Hsu, W. P.; Lee, Y. L.; Liou, S. H. *Appl. Surf. Sci.* **2006**, *252*, 4312.
(17) Murube, J.; Chen Zhuo, L.; Murube, E.; Montoya, C. *Complicaciones de las lentes de contacto*; Duran de la Colina, J. A., Ed.; Tecnimedia: Madrid, Spain, 1998; Chap. 7, p118.
(18) Baglioni, P.; Cestelli, G.; Dei, L.; Gabrielli, G. *J. Colloid Interface Sci.* **1985**, *104*, 143.

(19) Ries, H. E.; Matsumoto, M.; Uyeda, N.; Suito, E. *J. Colloid Interface Sci.* **1976**, *57*, 396.
(20) Müller-Landau, F.; Cadenhead, D. A. *Chem. Phys. Lipids.* **1979**, *25*, 299.
(21) Motomura, K.; Terazono, T.; Matuo, H.; Matuura, R. *J. Colloid Interface Sci.* **1976**, *57*, 52.
(22) Davies, J. T.; Rideal, E. K. *Interfacial Phenomena*; Academic Press: New York, 1961, p 265.
(23) Luckham, P.; Wood, J.; Frogatt, S.; Swart, R. *J. Colloid Interface Sci.* **1993**, *156*, 164–172.
(24) Fidelio, G. D.; Maggio, B.; Cumar, F. A. *Biochim. Biophys. Acta* **1986**, *854*, 231.
(25) Phillips, M. C.; Hauser, H. *J. Colloid Interface Sci.* **1974**, *49*, 31–39.
(26) Tajima, K.; Gershfeld, N. L. *Biophys. J.* **1978**, *22*, 489–500.
(27) Snick, A. F. M.; Kruger, A. J.; Joos, P. J. *J. Colloid Interface Sci.* **1978**, *66*, 435.
(28) Crisp, D. J. *Surface Chemistry (Suppl. Research)*; Butterworth: London, 1949; pp 17−35.
(29) Gaines, G., Jr. *Insoluble Monolayers at Liquid-Gas Interface*; Prigogine, I., Ed.; Interscience Publishers: New York, 1966; pp 281−291.
(30) Chifu, E.; Tomaia-Cotisel, M.; Ioanette, A. *Gazz. Chim. Ital.* **1979**, *109*, 397.
(31) Motomura, K.; Terazono, T.; Matu, H.; Matuura, R. *J. Colloid Interface Sci.* **1976**, *57*, 52.
(32) Albrecht, O.; Gruler, H.; Sackmann, E. *J. Colloid Interface Sci.* **1981**, *79*, 319.
(33) Nordli Borve, K. G. *Colloid Polym. Sci.* **1992**, *270*, 140.
(34) Miñones, J., Jr.; Miñones, J.; Rodríguez Patino, J. M.; Conde, O.; Iribarnegaray, E. *J. Phys Chem B.* **2003**, *107*, 4189.
(35) Handa, T.; Tomita, K.; Nakagaki, M. *Colloid Polym. Sci.* **1987**, *265*, 250.
(36) Defay, R.; Prigogine, I.; Bellmans, A.; Everett, D. E. *Surface Tension and Adsorption*; Longmans Green and Co.: London, 1966; p 71.
(37) Handa, T.; Nakagaki, M. *Colloid Polym. Sci.* **1979**, *257*, 374.
(38) Nakagaki, M.; Tomita, K.; Handa, T. *Biochemistry* **1985**, *24*, 4619.
(39) Gabrielli, G.; Maddii, A. *J. Colloid Interface Sci.* **1978**, *64*, 19.
(40) Malcolm., B. R. *Progress in Surface and Membrane Science*; Academic Press: New York, 1973; Vol. 7, p 223.
(41) Ries, H. E.; Walter, D. C. *J. Colloid Interface Sci.* **1961**, *16*, 361.
(42) Puggelli, M.; Gabrielli, G. *Colloid Polym. Sci.* **1983**, *261*, 82. Puggelli, M.; Gabrielli, G. *Colloid Polym. Sci.* **1987**, *263*, 879. Puggelli, M.; Gabrielli, G. *Colloid Polym. Sci.* **1987**, *265*, 432.
(43) Peng, J. B.; Barnes, G. T. *Langmuir* **1991**, *7*, 3090.
(44) Niccolai, A.; Baglioni, P.; Dei, L.; Gabrielli, G. *Colloid Polym. Sci.* **1989**, *267*, 262.
(45) Dörfler, H. D.; Koth, C.; Rettig, W. *Langmuir* **1995**, *11*, 4803.
(46) Dörfler, H. D.; Koth, C.; Rettig, W. *J. Colloid Interface Sci.* **1996**, *180*, 487.

JP103422G